Macromolecules

ARTICLE

pubs.acs.org/Macromolecules

Quantitative Analysis of the Effect of Azo Initiators on the Structure of α-Polymer Chain Ends in Degenerative Chain-Transfer-Mediated Living Radical Polymerization Reactions

Yasuyuki Nakamura,[†,‡] Yukie Kitada,[†] Yu Kobayashi,[§] Biswajit Ray,[§] and Shigeru Yamago*[,†,‡]

[†]Institute for Chemical Research, Kyoto University, Uji 611-0011, Japan

[‡]CREST, Japan Science and Technology Agency, and [§]Division of Molecular Materials Science, Graduate School of Science, Osaka City University, Osaka 558-8585, Japan

Supporting Information

ABSTRACT: The effects of azo initiators on the structures of the α-polymer chain ends in organotellurium-, organostibine-, organobismuthine-, and organoiodine-mediated living radical polymerizations (TERP, SBRP, BIRP, and IRP, respectively) and reversible addition−fragmentation chain transfer radical polymerization (RAFT) were quantitatively analyzed for the first time. These polymerization methods predominantly, or exclusively, follow the degenerative chain transfer (DT) mechanism for the activation and deactivation of dormant and radical species. An external radical species is required to initiate the polymerization under DT conditions, and the influx of radical species decreases the α-end-group fidelity. The effect was examined for polymerizations of styrene (St), *n*-butyl acrylate (BA), *N*-vinylpyrrolidone (NVP), methyl methacrylate (MMA), and isoprene (Ip) in the presence of different chain transfer agents (CTAs) and azo initiators, such as 2,2′-azobis(isobutyronitrile) (AIBN), 1,1′-azobis(cyclohexane-1-carbonitrile) (ACHN), and 1-[(1-cyano-1-methylethyl)azo]formamide (V-30), and the formed polymers **2** and **3**, which possess α-end structures derived from the CTA and azo initiator, respectively, were analyzed by using matrix-assisted laser desorption/ionization time-of-flight mass spectroscopy (MALDI-TOF MS). The amount of **3** was negligible when the rate of propagation (k_p) was sufficiently high, such as in the polymerizations of BA, MMA, and NVP. The formation of **3** was considerable when k_p was low, such as in the polymerizations of St and Ip, but was considerably reduced by carrying out the polymerization at high temperatures using an azo initiator decomposed at high temperatures. Furthermore, the formation of **3** was completely disappeared when the initiating radical was supplied by the reversible termination (RT) mechanism in TERP. The results indicate that α-polymer chain end structure is better controlled when both RT and DT are involved. The effect of azo initiator on the synthesis of a block copolymer was also examined, and pure diblock copolymer PMMA-*b*-PSt was obtained when both RT and DT were involved.

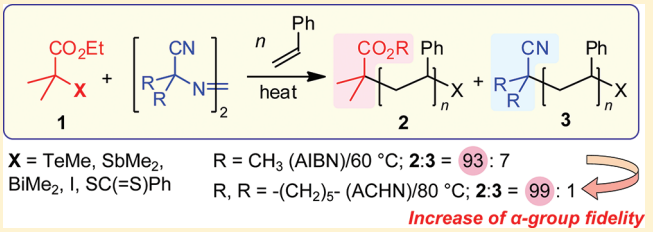

INTRODUCTION

Living radical polymerization (LRP) is a robust and versatile method for preparing structurally well-defined polymers with narrow molecular weight distributions (M_w/M_n), where M_w and M_n refer to the weight-average molecular weight and the number-average molecular weight, respectively.[1−3] LRP relies on the reversible generation of polymer-end radicals from dormant species (Scheme 1a), and this reversible radical generation decreases the concentration of radical species in solution, minimizing undesirable side reactions. Furthermore, the rapid deactivation makes it possible to elongate all of the polymer chains nearly equal rate, thus maintaining narrow M_w/M_n. So far, two activation/deactivation mechanisms have been reported. One is reversible termination (RT), in which dormant species P−X undergoes homolytic cleavage to give polymer end radical P$^•$ and persistent radical X$^•$ or its equivalent (Scheme 1b), and nitroxide-mediated polymerization (NMP)[4] and atom transfer radical polymerization (ATRP)[5−7] take place by this mechanism. The other is degenerative chain transfer (DT), in which a P′$^•$ undergoes a homolytic substitution reaction with dormant species P−X to give P$^•$ and P′−X dormant species (Scheme 1c). Reversible addition−fragmentation chain transfer (RAFT) radical polymerization proceeds exclusively via this mechanism.[8−10] Organoiodine-mediated living radical polymerization (IRP), in which moderate control of polymerization is possible, also proceeds via the DT mechanism.[11] Both RT and DT are involved in organocobalt-mediated polymerization, but the RT in coordinating solvent plays a more important role than the DT does.[12]

We have recently developed new LRP methods using organotellurium, organostibine, and organobismuthine compounds, which are designated as TERP, SBRP, and BIRP, respectively.[13−17] These methods are synthetically highly versatile and polymerize

Received: July 29, 2011
Revised: September 23, 2011
Published: October 13, 2011

varieties of monomer families in the presence of polar functional groups in a controlled manner. Furthermore, they can be used to prepare alternating,[18] block,[19−21] and end-functional polymers.[22−25] These methods predominantly proceed via the DT,[15,16,26,27] although RT is also involved to a small extent at elevated temperatures[14,28] or under photoirradiation.[17] The polymerization exclusively proceeds via the DT mechanism under mild thermal conditions upon addition of free radical initiators, such as azo initiators.[26] This condition is important from a practical point of view because the polymerization proceeds under mild thermal conditions without special equipment, such as a light source.

The DT mechanism is advantageous over the RT mechanism because the polymerization can proceed, in principle, at the same rate as conventional radical polymerization reactions.[29] In addition, one can enhance both the activation and deactivation rates simultaneously by using an appropriate capping group X because the activation and deactivation reactions are coupled to each other. On the other hand, the activation and deactivation rates are independent in the RT mechanism, and increasing the activation rate can decrease the control of the polymerization due to insufficient deactivation reaction.[30,31] However, the addition of radical initiators to generate initiating radical species is a potential disadvantage of DT mediated polymerization because the influx of radicals causes the formation of polymers possessing α-polymer chain end groups derived from the initiator (Scheme 2).[9] Therefore, complete control of the α-end structure is unattainable. The drawback of the radical initiator is more pronounced in block copolymer synthesis because homopolymers of the second monomer form due to the initiator-derived radicals. In addition, the use of radical initiators increases the formation of dead polymers as the number of polymer chains exceeds that of capping group X. Despite the apparent drawbacks, there are no reports on the quantitative analysis of the effects of the radical initiator on the α-polymer chain end structure so far.

Here we report quantitative analyses of the effects of free radical initiators on the structure of the α-polymer chain end in LRPs that proceed mainly or exclusively via the DT mechanism, namely, TERP, SBRP, BIRP, IRP, and RAFT. The effects of azo initiators on the polymerization of typical conjugated monomers, namely, styrene (St), *n*-butyl acrylate (BA), methyl methacrylate (MMA), and isoprene (Ip), as well as an unconjugated monomer, *N*-vinylpyrrolidone (NVP), were examined. After polymerization was carried out in the presence of chain transfer agent (CTA) **1** and an azo initiator, the amounts of polymers **2** and **3**, which were generated from **1** and the azo initiator, respectively, were analyzed by using matrix-assisted laser desorption/ionization time-of-flight mass spectroscopy (MALDI-TOF MS) after **2** and **3** were reduced to **4** and **5**, respectively (Scheme 3). The results indicated that, although the amount of **3** increased with an increase in the amount of the azo initiator, their effects on the α-polymer

Scheme 1. (a) General Mechanism of LRP, (b) Reversible Termination (RT), and (c) Degenerative Chain Transfer (DT) Mechanisms for the Activation/Deactivation Reaction of Dormant Species P−X and Polymer-End Radical P•[a]

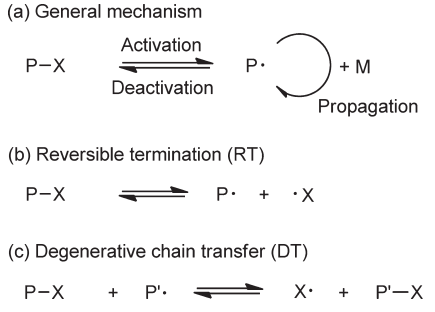

[a] P, M, and X denote polymer, monomer, and capping group, respectively.

Scheme 3. Effect of Azo Initiators on the α-Polymer Chain-End Structure in DT-Mediated LRP

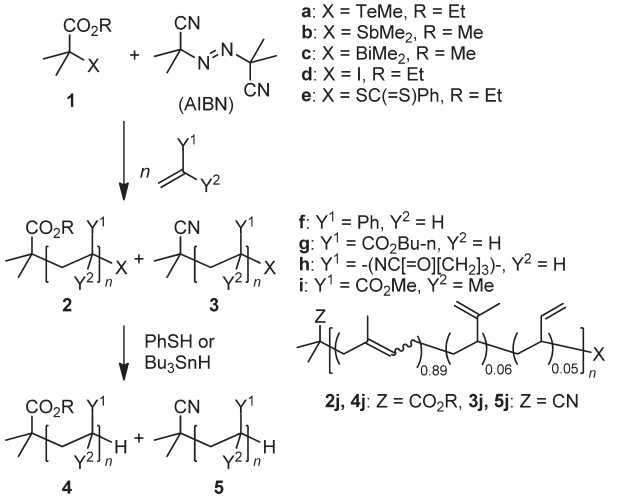

Scheme 2. Schematic Representation of the Effect of the Radical Initiator on Polymer-End Structures

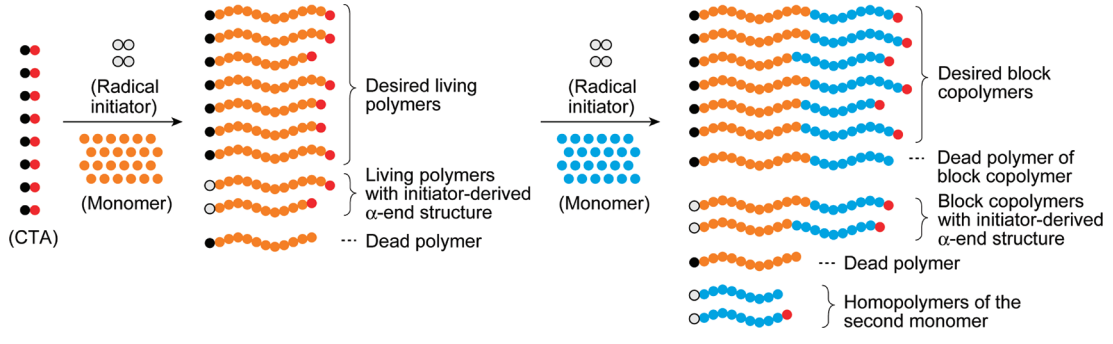

dx.doi.org/10.1021/ma201761q |*Macromolecules* 2011, 44, 8388–8397

chain-end structure were negligible in most cases, especially when the rate of polymerization was high, as with BA, NVP, and MMA polymerizations. However, a considerable effect was observed in the polymerization of St and Ip, the polymerizations of which proceed slowly. We developed a new general protocol to reduce the amount of undesired polymers for such cases on the basis of mechanistic analysis. We further confirmed the complete fidelity of the α-polymer chain end structures by generating initiating radicals under photoirradiation or high temperature from CTAs and dormant species by the RT mechanism without an azo initiator. The results clearly show that the presence of both DT and RT mechanisms is important for the complete control of the α-end structures. Detailed results are presented here.

EXPERIMENTAL SECTION

General. All reaction conditions dealing with air- and moisture-sensitive compounds were carried out in a dry reaction vessel under a nitrogen atmosphere. ^{1}H NMR (400 MHz) spectra were measured for a $CDCl_3$ solution of a sample and are reported in ppm (δ) from internal tetramethylsilane. Gel permeation chromatography (GPC) was performed on a machine equipped with two linearly connected polystyrene (PSt) mixed gel column (Shodex LF-604 or KF-804) at 40 °C using UV and RI detectors. The number-average molecular weight (M_n) is reported in g mol^{-1}. PSt, poly(*n*-butyl acrylate) (PBA), poly(methyl methacrylate) (PMMA), and polyisoprene (PIp) were analyzed by using $CHCl_3$ as an eluent, and poly(*N*-vinylpyrrolidone) (PNVP) was analyzed by using 0.01 M LiBr solution of DMF as an eluent. PSt and PIp were calibrated against PSt standards, and PBA, PNVP, and PMMA were against PMMA standards. MALDI-TOF MS spectra were recorded on a Bruker microflex spectrometer using positive reflector mode with 20 kV acceleration voltages. Samples were prepared by mixing a THF solution a polymer (10 mg/mL), dithranol (10 mg/mL), and silver trifluoroacetate (5 mg/mL, for PSt and PIp) or sodium trifluoroacetate (5 mg/mL, for others) in a ratio of 1:1:1. A 500 W high-pressure mercury lamp was used as a light source for photopolymerization. Cutoff filters (Asahi Techno Glass) were employed to control the intensity of light.[17] Theoretical calculations were performed with Gaussian 03 program. The geometry optimization was carried out using the B3LYP functional with the LANL2DZ(d,p) basis set for Te atom and the 6-31G(d) basis set for the others.

Materials. Unless otherwise noted, materials were obtained from commercial suppliers and were used as received. St, BA, MMA, and Ip were washed with 5% aqueous sodium hydroxide solution and were distilled over CaH_2. NVP was distilled over CaH_2. Azobis(isobutyronitrile) (AIBN), 1,1′-azobis(cyclohexane-1-carbonitrile) (ACHN), and 1-[(1-cyano-1-methylethyl)azo]formamide (V-30) was recrystallized from methanol and stored in a refrigerator. Chain transfer agents **1a**,[14] **1b**,[15] **1c**,[16] **1d**,[32] **1e**,[33] **11**,[14] and **12**[14] were synthesized as reported.

Synthesis of 13. To a solution of lithium diisopropylamide (85 mL, 0.78 mol/L in THF/hexane, 66 mmol) was added butyl propanoate (9.8 mL, 66 mmol) over 15 min at −78 °C under a nitrogen atmosphere, and the resulting solution was stirred at this temperature for 30 min. To this solution was added a solution of methyltellanyl bromide, which was prepared by mixing dimethylditelluride (3.18 mL, 30 mmol) and bromine (1.54 mL, 30 mmol) in THF (30 mL) at 0 °C, and then the resulting solution was gradually warmed to room temperature and stirred for 1.5 h. Degassed water was added, and the aqueous layer was separated under a nitrogen atmosphere. The remaining organic phase was washed successively with degassed, saturated aqueous NH_4Cl, and saturated aqueous NaCl solutions, dried over $MgSO_4$, and filtered under a nitrogen atmosphere. The solvent was removed under reduced pressure, followed by distillation (68−70 °C/1.1 mmHg), to give **13** in a 49% yield (8.8 g). ^{1}H NMR ($CDCl_3$): δ 0.94 (t, J = 7.6 Hz, 3H), 1.41 (m, 2H), 1.63 (m, 2H), 1.67 (d, J = 7.2 Hz, 3H), 2.14 (s, 3H, 3H), 3.69 (q, J = 7.2 Hz, 1H), 4.12 (q, J = 6.8 Hz, 2H). ^{13}C NMR ($CDCl_3$): δ −19.56, 11.43, 13.65, 18.78, 19.06, 30.56, 64.55, 175.94. HRMS (FAB) m/z: calcd for $C_8H_{16}O_2Te$ $[M]^+$, 274.0213; found 274.0219. IR (neat, cm^{-1}): 2959, 1717, 1458, 1377, 1323, 1246, 1192, 1126, 1072.

End-Group Analysis in St Polymerization. A solution of St (0.70 mL, 6.1 mmol), **1a** (36 μL, 0.20 mmol), and AIBN (3.3 mg, 0.020 mmol) was heated at 60 °C for 22 h under a nitrogen atmosphere in a glovebox. A small portion of the reaction mixture was removed, and the conversion of the monomer (96%) was determined by using ^{1}H NMR spectroscopy. The remaining reaction mixture was dissolved in trifluoromethylbenzene (1 mL). To the resulting solution was added benzenethiol (23 μL, 0.22 mmol).[34] The mixture was heated at 60 °C for 2 h and then poured into vigorously stirred methanol. The product was collected by suction filtration and dried in a vacuum at 50 °C. The number-average molecular weight (M_n = 3000) and MWD (M_w/M_n = 1.13) were determined by using gel permeation chromatography (GPC). The ratio of **5f** to the sum of **4f** and **5f** was determined to be 2% after correcting the raw data obtained from mass spectroscopy in relation to the ratio of the relative mass sensitivity of **4f** to **5f**, as shown below. The same experiments were carried out with the amount of AIBN in the range of 0.2−1.0 equiv versus **1a**.

End-Group Analysis in BA Polymerization. A solution of BA (1.00 mL, 7.0 mmol), **1a** (41 μL, 0.23 mmol), and AIBN (19.1 mg, 0.12 mmol) was heated at 60 °C for 1 h under a nitrogen atmosphere in a glovebox. A small portion of the reaction mixture was removed, and the conversion of the monomer (91%) was determined by using ^{1}H NMR spectroscopy. The remaining reaction mixture was dissolved in trifluoromethylbenzene (1 mL). To the resulting solution was added benzenethiol (28.6 μL, 0.27 mmol). The mixture was heated at 60 °C for 2 h, and then remaining monomer, solvent, and volatile compounds were removed in a vacuum. The M_n (3400) and M_w/M_n (1.13) were determined by GPC. The mass spectra revealed the no detectable formation of **3g**. The same experiments were carried out with the amount of AIBN in the range of 1.0 to 3.0 equiv versus **1a**.

End-Group Analysis in NVP Polymerization. A solution of NVP (0.39 mL, 3.7 mmol), **1a** (21 μL, 0.12 mmol), and AIBN (10.0 mg, 0.061 mmol) was heated at 60 °C for 2.5 h under a nitrogen atmosphere in a glovebox. A small portion of the reaction mixture was removed, and the conversion of the monomer (81%) was determined by ^{1}H NMR. The remaining reaction mixture was dissolved in trifluoromethylbenzene (1 mL). To the resulting solution was added benzenethiol (15 μL, 0.14 mmol). The mixture was heated at 60 °C for 2 h and then poured into vigorously stirred hexane. The product was collected by suction filtration and dried in a vacuum at 50 °C. The M_n (2200) and M_w/M_n (1.14) were determined by GPC. The ratio of **5h** to the sum of **4h** and **5h** was determined to be 0.4% after correcting the raw data obtained from mass spectroscopy in relation to the ratio of the relative mass sensitivity of **4h** and **5h** as shown below. The same experiments were carried out with the amount of AIBN in the range of 1−3 equiv versus **1a**.

End-Group Analysis in MMA Polymerization. A solution of MMA (1.0 mL, 9.4 mmol), **1a** (55 μL, 0.31 mmol), dimethylditelluride (33 μL, 0.31 mmol), and AIBN (26.0 mg, 0.16 mmol) was heated at 60 °C for 2 h under a nitrogen atmosphere in a groove box. A small portion of the reaction mixture was removed, and the conversion of the monomer (96%) was determined by ^{1}H NMR. The remaining reaction mixture was dissolved in trifluoromethylbenzene (2 mL). To the resulting solution was added benzenethiol (38.4 mg, 0.37 mmol). The mixture was heated at 60 °C for 2 h and then poured into vigorously stirred hexane. The product was collected by suction filtration and dried in a vacuum at 50 °C. The M_n (3500) and M_w/M_n (1.15) were determined by GPC. The ratio of **5i** to the sum of **4i** and **5i** was determined to be

0.4% after correcting the raw data obtained from the mass spectroscopy in relation to the ratio of the relative MS sensitivity of **4i** and **5i** as shown below. The same experiments were carried out with the amount of AIBN in the range of 1.0−3.0 equiv versus **1a**.

End-Group Analysis in Ip Polymerization. A solution of Ip (2.14 mL, 21 mmol), **1a** (125 μL, 0.71 mmol), and V-30 (10.0 mg, 0.071 mmol) in a Schlenk tube equipped with a Teflon stopcock was heated at 100 °C for 32 h under a nitrogen atmosphere. A small portion of the reaction mixture was removed, and the conversion of the monomer (78%) was determined by ^{1}H NMR.[35] The remaining reaction mixture was dissolved in trifluoromethylbenzene (1 mL). The resulting solution was added Bu_3SnH (230 μL, 0.86 mmol). The mixture was heated at 80 °C for 2 h, and then remaining volatile compounds were removed in a vacuum. The M_n (2800) and M_w/M_n (1.24) were determined by GPC. The ratio of **5j** to the sum of **4j** and **5j** was determined to be 0.5% after correcting the raw data obtained from the mass spectroscopy in relation to the ratio of the relative mass sensitivity of **4j** and **5j** as shown below. The same experiments were carried out with changing the amount of AIBN in the range 0.5 to 1 equiv versus **1a**.

Thermal Polymerization of St without AIBN.[14] A solution of St (3.0 mL, 26 mmol) and **1a** (151 μL, 0.86 mmol) was heated at 110 °C under a nitrogen atmosphere for 20 h. A small portion of the reaction mixture was removed, and the conversion of the monomer (92%) was determined by using ^{1}H NMR spectroscopy. The remaining reaction mixture was dissolved in trifluoromethylbenzene (3 mL). To the resulting solution was added benzenethiol (111 μL, 1.1 mmol) and AIBN (15 mg, 0.09 mmol), and the mixture was heated at 60 °C for 3 h. Then the solution was poured into vigorously stirred methanol. The product was collected by suction filtration and dried under reduced pressure at 50 °C. M_n (3600) and M_w/M_n (1.14) were determined by using GPC.

Typical Procedure for Photopolymerization.[17] A solution of St (1.0 mL, 8.7 mmol) and **1a** (51 μL, 0.29 mmol) was irradiated with an Hg lamp through a 610 nm short-wavelength cutoff filter at 50 °C under a nitrogen atmosphere for 27 h. A small portion of the reaction mixture was removed, and the conversion of St (93%) was determined by using ^{1}H NMR spectroscopy. The remainder of the reaction mixture was dissolved in trifluoromethylbenzene (1 mL). To the resulting solution was added benzenethiol (36 μL, 0.35 mmol), and the solution was irradiated with the same apparatus at 60 °C for 2 h and then was poured into vigorously stirred methanol. The product was collected by suction filtration and dried under reduced pressure at 50 °C. M_n (3400) and M_w/M_n (1.10) were determined by using GPC.

Photopolymerizations of MMA, NVP, and BA were carried with 700, 580, and 470 nm cutoff filters, respectively.

Synthesis of PMMA−TeMe Macroinitiator (14). A solution of MMA (2.4 mL, 22 mmol), **1a** (70 μL, 0.37 mmol), and AIBN (17 mg, 0.074 mmol) was heated at 60 °C for 3.5 h under a nitrogen atmosphere in a glovebox. A small portion of the reaction mixture was removed, and the conversion of the monomer (93%) was determined by using ^{1}H NMR spectroscopy. The remaining reaction mixture was dissolved in trifluoromethylbenzene (2 mL) and then poured into vigorously stirred degassed hexane. The product was collected by suction filtration and dried under reduced pressure. M_n (6050) and M_w/M_n (1.19) were determined by using GPC.

Synthesis of PMMA-*b*-PSt in the Presence of AIBN. A solution of **14** (340 mg, 56 μmol, M_n = 6050, M_w/M_n = 1.19), AIBN (4.6 mg, 28 μmol), and St (0.39 mL, 3.4 mmol) was heated at 60 °C for 8 h under a nitrogen atmosphere in a glovebox. A small portion of the reaction mixture was removed, and the conversion of the monomer (92%) was determined by using ^{1}H NMR spectroscopy. The remainder of the reaction mixture was dissolved in trifluoromethylbenzene (2 mL). To the resulting solution was added benzenethiol (6.3 μL, 0.06 mmol), and the solution was heated at 60 °C for 2 h and poured into vigorously stirred methanol. The crude product was collected by suction filtration and dried under vacuum at 50 °C to give 537 mg of the crude diblock copolymer (87% yield). M_n (12 700) and M_w/M_n (1.14) were determined by using GPC calibrated with PMMA standards.

Table 1. Relative MALDI-TOF MS Response Factor (f_s) of Polymers 4/5

polymer	f_s	polymer	f_s
4f	0.84	**4i**	1.04
4g	0.98	**4j**	0.42
4h	0.95		

The crude product (110 mg) in cyclohexane (7 mL) was sonicated for 10 min. The resulting suspension was filtered through a PTFE filter (pore size = 0.45 μm). The insoluble polymer was collected, and this procedure was repeated three times to give the purified block copolymer (101 mg) with M_n = 13 900 and M_w/M_n = 1.11. The filtrates were combined, and the solvent was evaporated to give PSt (7.7 mg) with M_n = 7400 and M_w/M_n = 1.21.

Synthesis of PMMA-*b*-PSt in the Absence of AIBN at 100 °C. A solution of **14** (M_n = 6050, M_w/M_n = 1.19, 255 mg, 0.042 mmol) and St (0.3 mL, 2.5 mmol) was heated at 100 °C for 18 h under a nitrogen atmosphere in a glovebox. A small portion of the reaction mixture was removed and dissolved in $CDCl_3$. The conversion of the monomer (88%) was determined by using ^{1}H NMR spectroscopy. The remaining reaction mixture was dissolved in trifluoromethylbenzene (2 mL). To the resulting solution was added benzenethiol (5.4 μL, 0.046 mmol), and the solution was irradiated with an Hg lamp through a 650 nm cutoff filter at 60 °C for 4 h and then was poured into vigorously stirred methanol. The product was collected by suction filtration and dried under reduced pressure at 50 °C. M_n (13 600) and M_w/M_n (1.14) were determined by using GPC calibrated with PMMA standards to give 402 mg of the crude diblock copolymer (83% yield).

Separation of the crude product (90 mg) gave the desired block copolymer (89 mg, M_n = 14 000, M_w/M_n = 1.11) and PSt (0.42 mg, M_n = 7400, M_w/M_n = 1.22).

Synthesis of PMMA-*b*-PSt under Photoirradiation. A solution of **14** (M_n = 6050, M_w/M_n = 1.19, 255 mg, 0.042 mmol) and St (0.3 mL, 2.5 mmol) was irradiated with an Hg lamp through a 650 nm cutoff filter at 70 °C for 15 h under a nitrogen atmosphere. A small portion of the reaction mixture was removed and dissolved in $CDCl_3$. The conversion of the monomer (89%) was determined by using ^{1}H NMR spectroscopy. The rest of the reaction mixture was dissolved in trifluoromethylbenzene (2 mL). To the resulting solution was added benzenethiol (5.4 μL, 0.046 mmol), and the solution was irradiated under the same conditions at 60 °C for 4 h and then was poured into vigorously stirred methanol. The product was collected by suction filtration and dried under reduced pressure at 50 °C. M_n (13 300) and M_w/M_n (1.11) were determined by using GPC calibrated with PMMA standards. No PSt homopolymer was detected after the extraction experiment used above.

Typical Procedure for the Determination of the Relative MS Sensitivity: PSts 4f and 5f. A mixture of **1a** (13.5 μL, 76 μmol), **6a**, (9.8 μL, 76 μmol), and St (5.3 mL, 4.6 mmol) was irradiated with an Hg lamp through a 610 nm cutoff filter at 50 °C for 60 h. The conversion of the monomer (93%) was determined by using ^{1}H NMR spectroscopy. The remaining reaction mixture was dissolved in trifluoromethylbenzene (1 mL). To the resulting solution was added benzenethiol (18.5 μL, 0.18 mmol), and the solution was irradiated at 60 °C for 2 h and then was poured into vigorously stirred methanol. The obtained polymer was analyzed by using MALDI-TOF MS, in which peaks corresponding to **4f** and **5f** were observed. The relative intensity ratio of **4f**/**5f** was

Table 2. Effect of AIBN in the Polymerization of St in the Presence of CTA 1a−1e[a]

entry	CTA	AIBN (equiv)	time (h)	conv (%)[b]	M_n(theo)	M_n(exp)[c]	M_w/M_n[c]	3 (%)[d]
1	**1a**	0.1	22	96	3100	3000	1.13	2
2	**1a**	0.2	22	96	3100	2800	1.15	4
3	**1a**	0.3	16	93	3000	2700	1.15	5
4	**1a**	0.5	13	99	3200	2900	1.16	7
5	**1a**	0.75	10	99	3200	2700	1.16	11
6	**1a**	1.0	8	95	3100	2800	1.22	12
7[e]	**1a**	0.5	18	97	5900	5200	1.21	10
8[f]	**1a**	0	27	93	3200	3400	1.10	0
9[g]	**1a**	0	20	92	3000	3600	1.14	0
10	**1b**	0.5	24	100	3300	3200	1.12	6
11	**1c**	0.5	16	92	3200	2900	1.17	6
12	**1d**	0.5	15	96	3000	3000	1.24	4
13	**1e**	0.5	48	63	2000	2100	1.18	6
14[h]	**1a**	0.5	8	92	2900	2700	1.18	1[j]
15[h]	**1e**	0.5	24	86	2700	2900	1.15	2[i]
16[j]	**1e**	0.5	12	90	2800	2600	1.16	<0.1

[a] A mixture of CTA (1 equiv), St (30 equiv), and AIBN (0.1−1equiv) was heated at 60 °C under a nitrogen atmosphere. [b] Monomer conversion was determined by using ^{1}H NMR spectroscopy. [c] Number-average molecular weight and M_w/M_n were determined by using GPC calibrated using PSt standards. [d] Molar ratio of **3** to the sum of **2** and **3** determined by using MALDI-TOF MS. The original data on mass intensities were corrected with the relative response factor (f_s). [e] 60 equiv of St was polymerized. [f] The polymerization was carried out under photoirradiation with a high-pressure Hg lamp with a >610 nm cutoff filter at 50 °C without AIBN. [g] The polymerization was carried out at 110 °C without AIBN. [h] Polymerization was carried out at 80 °C using ACHN instead of AIBN. [i] Amount of **10** (%) determined by MALDI-TOF-MS. MS data was corrected with f_s for **4f** and **5f**. [j] Polymerization was carried out at 100 °C using V-30 instead of AIBN.

determined to be 0.67 by comparing the peak intensities assuming equal initiation efficiency for **1a** and **6a**.

The same experiments were carried out with ratios of **1a**/**6a** of 0.5, 2.0, 9.0 and 19, and the ratios of **4f**/**5f** were determined to be 0.30, 1.6, 8.0, and 15.7 respectively. Linear approximation between the **1a**/**6a** and **4f**/**5f** ratios gave a relative MS sensitivity factor (f_s) of **4f**/**5f** of 0.84 (Table 1, entry 1).

The validity of f_s was confirmed by using the following control experiment: PSts **4f** (M_n = 2900, M_w/M_n = 1.10) and **5f** (M_n = 2600, M_w/M_n = 1.10) were independently prepared under thermal conditions without azo initiators starting from **1a** and **6a**, respectively. The same amount of **4f** and **5f** measured gravimetrically was mixed, and the resulting mixture was analyzed by using MALDI-TOF MS. The sample exhibited a relative peak intensity ratio of **4f**/**5f** of 0.78.

The same experiments were carried out with BA, NVP, MMA, and Ip, and the f_s values of **4g**/**5g**, **4h**/**5h**, **4i**/**5i**, and **4j**/**5j**, respectively, are summarized in Table 1.

RESULTS AND DISCUSSION

Effects of AIBN in St Polymerization. We first examined the effect of an azo initiator on the α-polymer chain-end structure in St polymerization. AIBN, the 10 h half-life decomposition temperature of which is 65 °C in toluene, was used as the azo initiator. The polymerization was carried out by heating a mixture of organotellurium CTA **1a** (1 equiv) and St (30 equiv) at 60 °C, with the amount of AIBN in the range of 0.10−1.0 equiv (Table 2, entries 1−6). The rate of monomer conversion increased with an increase in the amount of AIBN due to the increase in the concentration of the initiating radical species generated from AIBN. After nearly all of the St was consumed, the methyltellanyl ω-end group in **2f** and **3f** (Scheme 3) was reduced with benzenethiol to give **4f** and **5f** (Scheme 3),[34] respectively, which were analyzed by using GPC and MALDI-TOF MS (Table 2, entries 1−6). GPC analysis showed that structurally well-controlled PSts with the predicted M_n (2600−3000) from the ratio of St/**1a** and narrow M_w/M_n (1.13−1.22) formed in all cases. Although M_w/M_n slightly increased with an increase in the amount of AIBN, the level of the control remained excellent in all cases. The results indicate that AIBN has no significant effect on the overall control of M_w/M_n.

In MALDI-TOF MS spectra, however, a clear effect was observed on the basis of the two sets of molecular ion peaks for PSt: the major set corresponded to **4f** with a CTA-derived α-end structure, and the minor series corresponded to **5f** formed from an AIBN-derived radical species (Figure 1). The ratio of **5f**/(**4f** + **5f**) was 2% when 0.1 equiv of AIBN was employed (Table 2, entry 1), and it increased steeply with an increase in the amount of AIBN (entries 2−6 and Figure 2). The amount of **5f** was more than 10% when more than 0.75 equiv of AIBN was employed. In addition, the ratio of **5f** increased with an increase in the monomer/**1a** ratio (Table 2, entry 4 vs 7).[36,37]

On the other hand, polymerization under photoirradiation without AIBN exclusively gave **4f** as expected (Table 2, entry 8). Thermal polymerization without AIBN at 110 °C also gave **4f** exclusively (Table 2, entry 9).[14,17,38] Although autoinitiation is known to occur in St polymerization at high temperature,[39,40] PSt from autopolymerization could not be detected under the current conditions. The results clearly revealed the synthetic advantage of photochemical and thermal conditions without AIBN over thermal conditions in the presence of an azo initiator, especially for controlling the α-polymer chain end structure. In other words, care should be taken to avoid the formation of **3** especially when the targeted M_n is high, since 0.5−1.0 equiv of AIBN is employed in the polymerization of St under ambient thermal conditions.

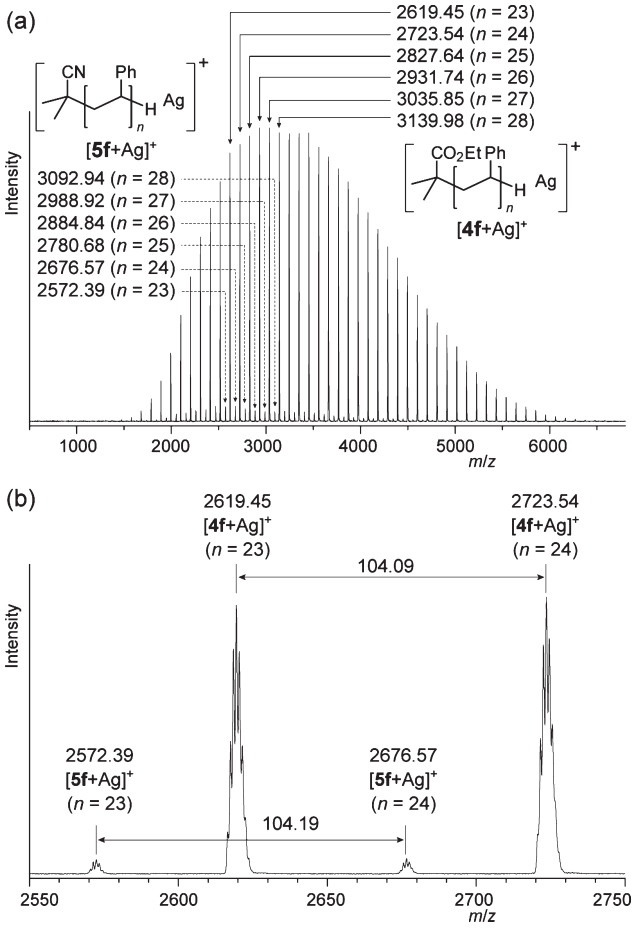

Figure 1. (a) Full and (b) partial MALDI-TOF MS spectra of PSt obtained from the polymerization of St (30 equiv) in the presence of **1a** and AIBN (0.3 equiv) (Table 2, entry 3). The peaks correspond to the silver ion adduct $[M + Ag]^+$.

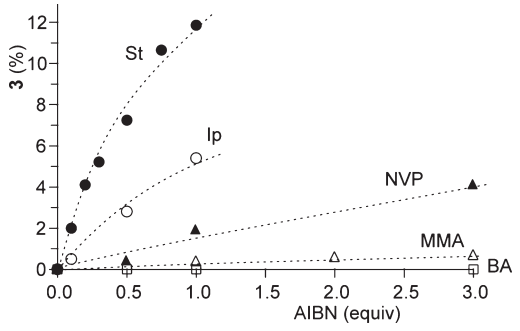

Figure 2. Ratio of **3** (%) versus the amount of AIBN (equiv) from the polymerizations of St (filled circles), Ip (open circles), NVP (filled triangles), MMA (open triangles), and BA (open squares).

The effect of the heteroatom group of the CTA was examined next using organostibine **1b**, organobismuthine **1c**, organoiodine **1d**, and RAFT agent **1e** in the presence of 0.5 equiv of AIBN at 60 °C (Table 2, entries 10−13). The polymerization rate was almost identical, and the monomer conversions became greater than 90% within 15 h, except under RAFT conditions, under which the conversion reached only 68% even after 48 h. All CTAs afforded well-controlled PSts with the predicted M_n from St/**1** ratio and narrow M_w/M_n (1.12−1.24). The amount of **5f** formed (4%−6%) was the same as that using organotellurium CTA **1a** (7%) within experimental error. The insensitivity of the capping group X must be due to the sufficiently high reactivity of X group studied here toward the chain transfer reaction (see below).

Scheme 4. Mechanism for Formation of AIBN-Derived Polymer 3[a]

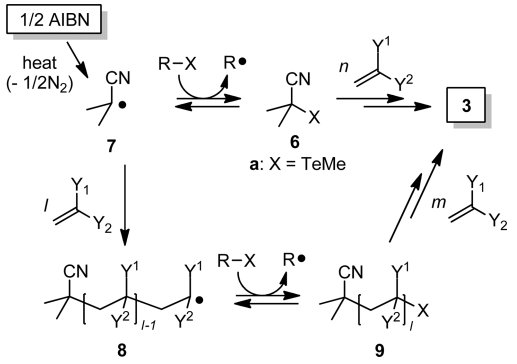

[a] R−X refers to either the CTA or a dormant species in the reaction mixture.

Chart 1. Structure of PSt 10 Derived from ACHN

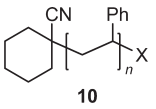

10

Polymer **3** formed via two pathways (Scheme 4). One pathway involves direct chain transfer reaction of AIBN-derived radical **7** with either CTA or dormant species giving cyano-substituted CTA **6**. Since **6** is an excellent CTA,[16,20,26,41] it undergoes DT-mediated polymerization to give **3**. The other pathway proceeds via initial addition of **7** to the monomer to give oligomer radical **8**, which undergoes chain transfer with either the CTA or a dormant species to give oligomeric dormant species **9**. Subsequent DT-mediated polymerization affords **3**. The mechanism indicates that the amount of **7** presents during the polymerization determines the amount of **3**, when chain transfer from **7** and **8** to CTA or dormant species is efficient. Therefore, the amount of **3** increased with an increase in the amount of AIBN. In addition, since the polymerization required longer periods with an increase in the amount of monomer, the amount of **3** formed increased when the ratio of monomer/**1** increased.

The negligible effect of the capping group X in **1** was attributed to the high reactivities of the heteroatom species toward the chain transfer reaction. Although the chain transfer reaction in St polymerization is the fastest with the RAFT polymer end (X = SC(=S)Ph, $k_{ex} = 2.0 \times 10^6$ mol L^{-1} at 40 °C),[42] followed by that with the BIRP (X = $BiMe_2$, $k_{ex} = 4.6 \times 10^4$ mol L^{-1} at 60 °C),[16] SBRP (X = $SbMe_2$, $k_{ex} = 1.1 \times 10^4$ mol L^{-1} at 60 °C),[27] TERP (X = TeMe, $k_{ex} = 5.8 \times 10^3$ mol L^{-1} at 60 °C),[43] and then IRP ones (X = I, $k_{ex} = 3.4 \times 10^2$ mol L^{-1} at 60 °C),[44] the rate of the chain transfer with the IRP polymer end is still sufficiently high to achieve an effective exchange reaction. The results indicated that the amount of azo initiator and the time required for the polymerization were the primary factors in the formation of **3**.

dx.doi.org/10.1021/ma201761q |*Macromolecules* 2011, 44, 8388–8397

Table 3. Effect of AIBN on the Polymerization of Various Monomers in the Presence of 1a[a]

entry	monomer	AIBN (equiv)	time (h)	conv (%)[b]	M_n(theo)	M_n(exp)[c]	M_w/M_n[c]	3 (%)[d]
1	BA	0.5	0.9	91	3200	3400	1.13	<0.1
2	BA	1.0	0.7	98	4000	4100	1.15	<0.1
3	BA	3.0	0.4	91	3700	3900	1.14	<0.1
4	BA[e]	0	3	92	3800	4100	1.16	0
5	NVP	0.5	2.5	81	2800	2200	1.14	0.4
6	NVP	1.0	2	86	2800	2700	1.09	2
7	NVP	3.0	1.5	84	2900	3200	1.11	4
8	NVP[e]	0	8	75	2700	2300	1.14	0
9	MMA	1.0	1.5	98	3100	4800	1.24	0.4
10	MMA	3.0	1.5	100	3100	5000	1.21	0.7
11	MMA[e]	0	13.5	97	3200	3700	1.17	0
12	Ip[f]	0.1	32	78	1700	2800	1.24	0.5
13	Ip[f]	0.5	43	62	1400	2100	1.31	3
14	Ip[f]	1.0	52	80	1800	2400	1.32	5

[a] A mixture of **1a**, monomer (30 equiv), and AIBN (0.5−3 equiv) was heated at 60 °C under a nitrogen atmosphere. [b] Monomer conversion was determined by using ^{1}H NMR spectroscopy. [c] Number-average molecular weight and M_w/M_n were determined by GPC calibrated using PSt or PMMA standards. [d] Molar ratio of **3** to the sum of **2** and **3** determined by MALDI-TOF MS. [e] The polymerization was carried out under photoirradiation. See Supporting Information for the details. [f] A mixture of **1a**, Ip (30 equiv), and V-30 (0.1−1 equiv) was heated at 100 °C under a nitrogen atmosphere.

The above mechanistic interpretation indicates that the amount of the azo-derived polymer, such as **3**, should decrease if the polymerization is carried out at high temperature by employing an azo initiator that decomposes at higher temperature. This is because polymerization will go to completion faster due to the higher temperature while the influx of the radical species from the initiator remains slow. Indeed, the formation of the ACHN-derived polymer **10** (Chart 1) was 1% when TERP of St (30 equiv) was carried out at 80 °C with **1a** and ACHN (0.5 equiv; 10 h half-life decomposition temperature = 87 °C in toluene) (Table 2, entry 14). The formation of **10** was also negligible (2%) when RAFT of St was examined with **1e** and ACHN at 80 °C (Table 2, entry 15). When RAFT of St (30 equiv) was carried out at 100 °C with **1e** and V-30 (0.5 equiv; 10 h half-life decomposition temperature = 104 °C in toluene), virtually complete control of α-end structure was achieved (<0.1% of **3**) (Table 2, entry 16).[45] In addition, while RAFT usually proceeds slowly and does not go to high monomer conversion, the monomer conversion reached high (90%) within 12 h. Therefore, the polymerization at high temperature is advantageous not only for the high control of α-end structure but also the polymerization efficiency. These conditions should be also effective in SBRP, BIRP, and IRP.

Effects of AIBN on the Polymerizations of BA, NVP, MMA, and Ip. The effects of AIBN on the polymerizations of BA, NVP, MMA, and Ip were examined next. Bulk polymerization of BA (30 equiv) was carried out at 60 °C in the presence of **1a** by varying the amount of AIBN from 0.50 to 3.0 equiv. Polymerization was complete within 1 h in all cases (Table 3, entries 1−3). The faster monomer conversion for BA polymerization compared with that for St polymerization is consistent with the higher propagation rate constant for the former ($k_p = 3.4 \times 10^4$ L mol^{-1} s^{-1} at 60 °C)[46] compared with the latter ($k_p = 3.4 \times 10^2$ L mol^{-1} s^{-1} at 60 °C).[47] GPC analysis indicated the formation of well-controlled PBA with the predicted M_n and narrow M_w/M_n (<1.2) in all cases. In the mass spectra, **5g** was not observed within experimental error even when 3.0 equiv of AIBN was employed (Figure 2), and only a tiny amount of initiating radical was sufficient to attain high monomer conversion. Since less than 0.5 equiv of an azo initiator is usually employed in acrylate polymerization under TERP conditions, the results indicate that virtually complete control of the α-end structure is possible in acrylate polymerization.

Polymerization of NVP was examined next under the same conditions as those for BA polymerization. Polymerization completed within 3 h at 60 °C and gave structurally well-controlled PNVP with the predicted M_n and narrow M_w/M_n (<1.14). The amount of **5h** was negligible (0.4%) when 0.5 equiv of AIBN was employed (Table 3, entry 5) but slightly increased (2%−4%) when the amount of ABIN was increased to 1.0 and then to 3.0 equiv (Table 3, entries 6 and 7, and Figure 2). Since k_p for NVP (2.5×10^3 L mol^{-1} s^{-1} at 60 °C)[48] is in between those for BA and St, the results are consistent with the monomer reactivities. The polymerization of NVP usually proceeds with less than 0.5 equiv of ABIN, and the effect of AIBN on the α-end structure should be marginal even when the target M_n is increased.

Polymerization of MMA was examined in the presence of dimethyl ditelluride (1.0 equiv)[21,43] under the same conditions as those for BA.[26] Despite the lower k_p for MMA (8.4×10^2 L mol^{-1} s^{-1} at 60 °C)[49] compared with that for NVP, the polymerization time was similar to that of NVP, and well-controlled PMMAs with predicted M_n and narrow M_w/M_n (<1.24) were obtained in all cases. From analysis of MALDI-TOF MS spectra, PMMA **4i**, derived from **1a**, predominantly formed, and the amount of AIBN-derived **5i** was negligible. Although the formation of **5i** slightly increased when more AIBN was used, only 0.7% of **5i** formed even when 3.0 equiv of AIBN was added. We have already reported that the addition of ditelluride increases the rate of polymerization of MMA by increasing the rate of activation of the dormant species.[43] Therefore, the increased polymerization rate and the decrease in polymerization time are the major reasons for the negligible amount of **5i**.

Polymerizations of BA, NVP, and MMA were carried out under photoirradiation without azo initiators. **4** (Scheme 3)

Chart 2. Structure of Organotellurium CTAs

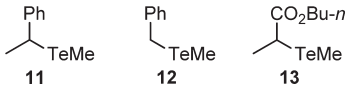

Table 4. Structural Effect of Organoheteroatom CTAs in St Polymerization[a]

entry	CTA	time (h)	conv (%)[b]	M_n (theo)	M_n (exp)[c]	M_w/M_n[c]	3 (%)[d]
1	**11**	7	93	2900	2200	1.16	7
2	**12**	17	92	2900	3600	1.23	11
3	**13**	15	100	3400	3300	1.41	14

[a] A mixture of **1**, monomer (30 equiv), and AIBN (0.5 equiv) was heated at 60 °C under a nitrogen atmosphere. [b] Monomer conversion was determined by using ^{1}H NMR spectroscopy. [c] Number-average molecular weight and M_w/M_n were determined by GPC calibrated using PSt standards. [d] Molar ratio of **3** to the sum of PSt having CTA derived α-chain end and **3** determined by using MALDI-TOF MS.

Table 5. Bond Dissociation Energy of C−Te Bond of Organotellurium CTAs

CTA	BDE, kJ mol^{-1}	CTA	BDE, kJ mol^{-1}
1a[a]	122	**12**	143
6a	120	**13**[a]	152
11	124		

[a] BDE was calculated using methyl ester as a model compound.

exclusively formed in all cases (Table 3, entries 4, 8, and 11), showing that the involvement of RT mechanism for the activation of the dormant species is advantageous in TERP.

Next, the polymerization of Ip was examined in the presence of **1a**. Since the polymerization did not proceed efficiently at 60 °C due to the low k_p of Ip (1.3×10^2 L mol^{-1} s^{-1} at 60 °C),[50] it was carried out at 100 °C with V-30 (0.1−1.0 equiv) as an initiator. The monomer conversion reached 62%−80% after 32−52 h, and PIps with M_n = 2100−2800 and M_w/M_n = 1.24−1.32 were obtained (Table 3, entries 12−14). The formation of **5j** was lower than that of **5f** in St polymerization, and **4j** formed predominantly. The amount of **5j** was at most 5% even when 1.0 equiv of V-30 was added. V-30 decomposes at 100 °C at a rate similar to that of AIBN at 60 °C. However, since only one initiating radical is generated from one V-30 molecule, whereas two radicals are generated from one AIBN molecule, the observed difference must be due to the amount of radicals from azo initiators during the polymerization period.

Structural Effect of the CTAs. The effects of the structure of the CTA on the control of the α-end structure were investigated by using organotellurium CTAs **11**−**13** (Chart 2 and Table 4). St polymerization was performed with each CTA in the presence of 0.5 equiv of AIBN at 60 °C. From GPC analysis, the level of control using **11** was excellent, as in the case of **1a**, but that using **12** and **13** was lower, with the control using **12** being greater than that using **13**. The amount of **5f** was 7%, 11%, and 14% when **11**, **12**, and **13** were used, respectively. The results show that the structure of the CTA considerably affects the control of both M_w/M_n and the α-end structure.

Scheme 5. Effect of AIBN on the Synthesis of PMMA-*b*-PSt

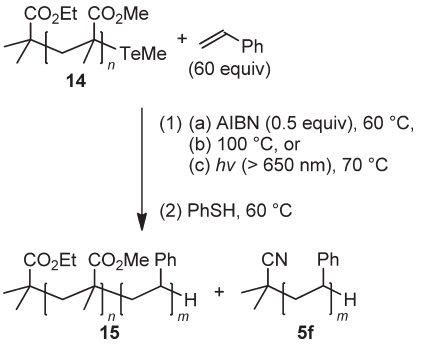

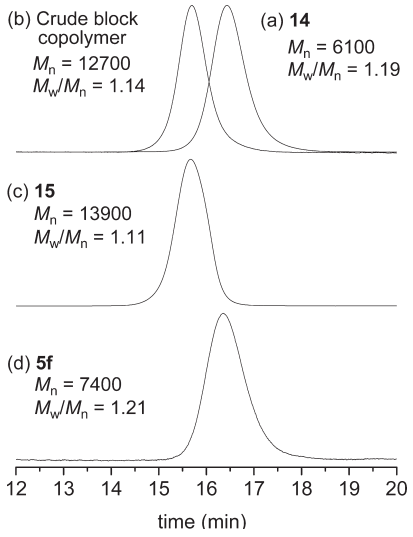

Figure 3. GPC traces of PMMA-*b*-PSt synthesized from PMMA−TeMe and St in the presence of 0.5 equiv of AIBN: (a) macroCTA **14**, (b) crude block copolymer, (c) purified block copolymer **15**, and (d) extracted PSt **5f**.

The lower control of M_w/M_n by using **12** and **13** is rationalized by the slower generation of initiating radicals from **12** and **13** than that from **1** and **11**. Radicals generated from **12** and **13** are ca. 20 and 30 kJ/mol less stable than those generated from **1a**, respectively, on the basis of the bond dissociation energies of the C−Te bond, whereas those generated from **6a** and **11** are very similar to that of **1a** (Table 5). As the chain transfer reactions of the heavier heteroatom compounds have low activation energies,[16,27,38,42,44] the bond dissociation energy strongly reflects the kinetic reactivity of the CTAs in the generation of the corresponding radicals. Therefore, the generation of initiating radicals from CTAs possessing higher bond dissociation energy is less efficient. This leads to the slow generation of radicals from CTA molecules, leading to a decrease in the control of M_w/M_n as well as an increase in the amount of **5f**.

Effects of AIBN on Block Copolymer Synthesis. The effects of azo initiators on block copolymer synthesis were examined. PMMA-TeMe macroCTA **14** (M_n = 6100, M_w/M_n = 1.19) and St (60 equiv) were heated in the presence of 0.5 equiv of AIBN at 60 °C. The desired block copolymer PMMA-*b*-PSt with M_n = 12 700 and narrow M_w/M_n (= 1.14) formed (Scheme 5 and Figure 3a and 3b). However, extractive purification revealed that a

dx.doi.org/10.1021/ma201761q |*Macromolecules* 2011, 44, 8388–8397

small amount (11%) of PSt homopolymer (M_n = 7400, M_w/M_n = 1.21) formed from an AIBN-derived radical (Figure 3d). The result is consistent with the observed effects of AIBN on St polymerization mentioned above.

The block copolymer was also synthesized under thermal conditions at 100 °C or photoirradiation without AIBN. Structurally well-controlled PMMA-*b*-PSts with narrow M_w/M_n (∼1.14) were obtained under both conditions on the basis of GPC analyses. Further analysis revealed that amount of the PSt homopolymer was negligible (0.7%) under thermal conditions and that no homopolymer was detected under photochemical conditions. Since purification of block copolymers is difficult in many instances, the synthesis of pure block copolymer is practically important. Therfore, polymerization under thermal and photochemical conditions without azo initiators is advantageous for the precision synthesis of block copolymers.

■ CONCLUSION

The effects of azo initiators on the structure of the α-polymer chain end in the DT-mediated LRP, namely, TERP, SBRP, BIRP, IRP, and RAFT, of BA, NVP, MMA, St, and Ip were quantitatively studied by using MALDI-TOF MS. The formation of **3** with an azo initiator-derived chain end structure was almost negligible in most cases. However, it became high in the polymerization of St and Ip, especially when a large amount of azo initiator was employed. Thus, the amount of azo initiator should be carefully controlled to attain high control of the α-end structure. Increased control of the α-end was attained by carrying out the polymerization at high temperature with an azo initiator that decomposes at higher temperatures or by using the RT mechanism to activate the dormant species. Although the effects of the capping agent on the structure were small among TERP, SBRP, BIRP, IRP, and RAFT, those of the initiating radical part were large. Therefore, CTAs must be carefully chosen for high control of both M_w/M_n and the α-polymer chain end group.

■ ASSOCIATED CONTENT

Supporting Information. Determination of relative MS response factor, MALDI-TOF MS analyses for the polymerization mixture forming **4** and **5**, analysis of PSt **5f** formed in PMMA-*b*-PSt synthesis, and ^{1}H and ^{13}C NMR spectra of compound **13**. This material is available free of charge via the Internet at http://pubs.acs.org.

■ AUTHOR INFORMATION

Corresponding Author
*E-mail: yamago@scl.kyoto-u.ac.jp.

■ ACKNOWLEDGMENT

This work was partly supported by the Core Research for Evolution Science and Technology (CREST) of the Japan Science and Technology Agency. Computation time was provided by the Super Computer Laboratory, Institute for Chemical Research, Kyoto University.

■ REFERENCES

(1) Matyjaszewski, K.; Davis, T. P. *Handbook of Radical Polymerization*; Wiley-Interscience: New York, 2002.
(2) Moad, G.; Solomon, D. H. *The Chemistry of Radical Polymerization*; Elsevier: Amsterdam, 2006.
(3) Matyjaszewski, K.; Gnanou, Y.; Leibler, L. *Macromolecular Engineering*; Wiley-VCH: Weiheim, 2007.
(4) Hawker, C. J.; Bosman, A. W.; Harth, E. *Chem. Rev.* **2001**, *101*, 2921–2990.
(5) Matyjaszewski, K.; Xia, J. *Chem. Rev.* **2001**, *101*, 2921–2990.
(6) Ouchi, M.; Terashima, T.; Sawamoto, M. *Acc. Chem. Res.* **2008**, *41*, 1120–1132.
(7) Ouchi, M.; Terashima, T.; Sawamoto, M. *Chem. Rev.* **2009**, *109*, 4963–5050.
(8) Lowe, A. B.; McCormick, C. L. *Prog. Polym. Sci.* **2007**, *32*, 283–351.
(9) Moad, G.; Rizzardo, E.; Thang, S. H. *Acc. Chem. Res.* **2008**, *41*, 1133–142.
(10) Moad, G.; Rizzardo, E.; Thang, S. H. *Aust. J. Chem.* **2009**, *62*, 1402–1472.
(11) David, G.; Boyer, C.; Tonnar, J.; Ameduri, B.; Lacroix-Desmazes, P.; Boutevin, B. *Chem. Rev.* **2006**, *106*, 3936–3962.
(12) Debuigne, A.; Poli, R.; Jérôme, C.; Jérôme, R.; Detrembleur, C. *Prog. Polym. Sci.* **2009**, *34*, 211–239.
(13) Yamago, S. *Chem. Rev.* **2009**, *109*, 5051–5068.
(14) Yamago, S.; Iida, K.; Yoshida, J. *J. Am. Chem. Soc.* **2002**, *124*, 2874–2875.
(15) Yamago, S.; Ray, B.; Iida, K.; Yoshida, J.; Tada, T.; Yoshizawa, K.; Kwak, Y.; Goto, A.; Fukuda, T. *J. Am. Chem. Soc.* **2004**, *126*, 13908–13909.
(16) Yamago, S.; Kayahara, E.; Kotani, M.; Ray, B.; Kwak, Y.; Goto, A.; Fukuda, T. *Angew. Chem., Int. Ed.* **2007**, *46*, 1304–1306.
(17) Yamago, S.; Ukai, Y.; Matsumoto, A.; Nakamura, Y. *J. Am. Chem. Soc.* **2009**, *131*, 2100–2101.
(18) Mishima, E.; Yamago, S. *Macromol. Rapid Commun.* **2011**, *32*, 893–898.
(19) Mishima, E.; Yamada, T.; Watanabe, H.; Yamago, S. *Chem.—Asian J.* **2011**, *6*, 445–451.
(20) Ray, B.; Kotani, M.; Yamago, S. *Macromolecules* **2006**, *39*, 5259–5265.
(21) Yamago, S.; Iida, K.; Yoshida, J. *J. Am. Chem. Soc.* **2002**, *24*, 13666–13667.
(22) Kayahara, E.; Yamada, H.; Yamago, S. *Chem.—Eur. J.* **2011**, *17*, 5271–5279.
(23) Yamago, S.; Yamada, T.; Togai, M.; Ukai, Y.; Kayahara, E.; Pan, N. *Chem.—Eur. J.* **2009**, *15*, 1018–1029.
(24) Yamago, S.; Kayahara, E.; Yamada, H. *React. Funct. Polym.* **2009**, *69*, 416–423.
(25) Yamada, T.; Mishima, E.; Ueki, K.; Yamago, S. *Chem. Lett.* **2008**, 650–651.
(26) Goto, A.; Kwak, Y.; Fukuda, T.; Yamago, S.; Iida, K.; Nakajima, M.; Yoshida, J. *J. Am. Chem. Soc.* **2003**, *125*, 8720–8721.
(27) Kwak, Y.; Goto, A.; Fukuda, T.; Yamago, S.; Ray, B. *Z. Phys. Chem.* **2005**, *219*, 283–293.
(28) Yamago, S.; Iida, K.; Nakajima, M.; Yoshida, J. *Macromolecules* **2003**, *36*, 3793–3796.
(29) Barner-Kowollik, C.; Buback, M.; Charleux, B.; Coote, M. L.; Drache, M.; Fukuda, T.; Goto, A.; Klumperman, B.; Lowe, A. B.; McLeary, J. B.; Moad, G.; Monteiro, M. J.; Sanderson, R. D.; Tonge, M. P.; Vana, P. *J. Polym. Sci., Part A: Polym. Chem.* **2006**, *44*, 5809–5831.
(30) Siegenthaler, K. O.; Studer, A. *Macromolecules* **2006**, *39*, 1347.
(31) Queffelec, J.; Gaynor, S. G.; Matyjaszewski, K. *Macromolecules* **2000**, *33*, 8629.
(32) Ando, T.; Kamigaito, M.; Sawamoto, M. *Macromolecules* **2000**, *33*, 2819–2824.
(33) Chong, B. Y. K.; Krstina, J.; Le, T. P. T.; Moad, G.; Postma, A.; Rizzardo, E.; Thang, S. H. *Macromolecules* **2003**, *36*, 2256–2272.
(34) Yamago, S.; Matsumoto, A. *J. Org. Chem.* **2008**, *73*, 7300–7304.
(35) Wegrzyn, J. K.; Stephan, T.; Lau, R.; Grubbs, R. B. *J. Polym. Sci., Part A: Polym. Chem.* **2005**, *43*, 2977–2984.

(36) While the formation of **5f** indicates the formation dead polymers derived from polymer-end radicals (Scheme 2), we could not detect the corresponding species, presumably a coupling product. It is better to assume that the formation of uncharacterized dead polymers also increases with the increase of the formation of **5f**.

(37) Polymers of low molecular weight (oligomers) may be soluble in the solvent used for precipitation and be removed from the MS sample. However, the amount of **5f** did not change before and after the precipitation.

(38) Kwak, Y.; Goto, A.; Fukuda, T.; Kobayashi, Y.; Yamago, S. *Macromolecules* **2006**, *39*, 4671–4679.

(39) Mayo, F. R. *J. Am. Chem. Soc.* **1968**, *90*, 1289–1295.

(40) Kirchner, V. K. *Makromol. Chem.* **1996**, *96*, 179–186.

(41) Chiefari, J.; Chong, B. Y. K.; Ercole, F.; Krstina, J.; Jeffery, J.; Le, T. P. T.; Mayadunne, R. T. A.; Meijs, G. F.; Moad, C. L.; Moad, G.; Rizzardo, E.; Thang, S. H. *Macromolecules* **1998**, *31*, 5559–5562.

(42) Goto, A.; Sato, K.; Tsujii, Y.; Fukuda, T.; Moad, G.; Rizzardo, E.; Thang, S. H. *Macromolecules* **2001**, *34*, 402–408.

(43) Kwak, Y.; Tezuka, M.; Goto, A.; Fukuda, T.; Yamago, S. *Macromolecules* **2007**, *40* (6), 1881–1885.

(44) Goto, A.; Ohno, K.; Fukuda, T. *Macromolecules* **1998**, *31*, 2809–2814.

(45) V-30 is soluble in organic solvent, and the reaction mixture was homogeneous under the current conditions.

(46) Lyons, R. A.; Hutovic, J.; Piton, M. C.; Gilbert, R. G. *Macromolecules* **1998**, *29*, 1918–1927.

(47) Gilbert, R. G. *Pure Appl. Chem.* **1996**, *68*, 1491–1494.

(48) Stach, M.; Lacík, I.; Charvát, J., D.; Buback, M.; Hesse, P.; Hutchinson, R. A.; Tang, L. *Macromolecules* **2008**, *41*, 5174–5185.

(49) Beuermann, S.; Buback, M.; Davis, T. P.; Gilbert, R. G.; Hutchinson, R. A.; Olaj, O. F.; Russell, G. T.; Schweer, J.; van Herk, A. M. *Macromol. Chem. Phys.* **1997**, *198*, 1545–1560.

(50) Kamachi, M.; Kajiwara, A. *Macromolecules* **1996**, *29*, 2378–2382.